Bioactive Materials 44 (2025) 256–268

Contents lists available at ScienceDirect

Bioactive Materials

journal homepage: www.keaipublishing.com/en/journals/bioactive-materials

# An injectable hyaluronic acid/lithium calcium silicate soft tissue filler with vascularization and collagen regeneration

Jinzhou Huang [a,b,1], Jianmin Xue [a,b,1], Jimin Huang [a,b], Xinxin Zhang [a,b], Hongjian Zhang [a,b], Lin Du [a,b], Dong Zhai [a], Zhiguang Huan [a,b], Yufang Zhu [a,b,*], Chengtie Wu [a,b,**]

[a] State Key Laboratory of High Performance Ceramics and Superfine Microstructure, Shanghai Institute of Ceramics, Chinese Academy of Sciences, 1295 Dingxi Road, Shanghai, 200050, PR China

[b] Center of Materials Science and Optoelectronics Engineering, University of Chinese Academy of Sciences, 19A Yuquan Road, Beijing, 100049, PR China

ARTICLE INFO

*Keywords:*
Lithium calcium silicate
Microspheres
Injectable filler
Collagen secretion
Vascular regeneration

ABSTRACT

The significance of collagen and vascular in skin augmentation have been recognized in recent years. However, current skin tissue fillers, *e.g.* hyaluronic acid (HA) or HA-based hydrogel, fail to meet the perfect augmentation requirements due to their inadequate long-term support effect and the lack of tissue-inducing activity. Herein, an injectable skin filler containing hyaluronic acid (HA) hydrogel and lithium calcium silicate (LCS, $Li_2Ca_4Si_4O_{13}$) bioceramic microspheres was developed for skin tissue fillers, owing to the excellent biological function of silicate bioceramics. The HA-LCS fillers could be easily injected through a tiny standard medical needle (27 G) with force of less than 36 N, and showed good biocompatibility both *in vitro* and *in vivo*. Furthermore, the bioactive ions released from HA-LCS fillers significantly enhanced the expression of vascularization-related genes and collagen-related genes. Importantly, the HA-LCS fillers not only stimulated the regeneration of mature blood vessels, but also promoted collagen secretion in dermal skin and filling area. This study not only presented an injectable filler with enhanced regeneration of blood vessels and collagen, but also provided a new strategy for developing tissue-induced fillers based on bioactive components of silicate bioceramics.

## 1. Introduction

With age and exposure to external stimulations, the gradual increase in loss or damage of skin collagen leads to the development of wrinkles and sagging [1,2]. Soft tissue fillers have been extensively studied for their anti-wrinkle effects in cosmetic medicine over the past few decades [3]. Among them, hyaluronic acid (HA), an injectable soft tissue filler, has significantly advanced the field of soft tissue augmentation [4,5]. HA injection fillers offer several advantages such as simple surgical procedures, minimal invasiveness, low risk, and shorter recovery time. Consequently, they have become the most popular choice for facial aesthetic injections nowadays [6,7]. However, HAfillers only provide a physical filling effect for a short time due to its rapid degradation rate, resulting in frequent repeat injections to maintain supporting effect [8,9].

Recently, several tissue-induced fillers containing hydroxyapatite (HAP), polylactic acid (PLA), polycaprolactone (PCL) microspheres have been developed [10–12]. These tissue-induced fillers not only provide enhanced support function, but also induce the collagen production through cellular activation by microspheres following degradation of the hydrogel carrier [13,14]. Regrettably, these fillers still exhibit some adverse effects as the microspheres possess exceptional stability that impedes their degradation over an extended period of time. The prolonged presence of chronic inflammation in the filling area may lead to the formation of granulomas and other tissue problems [15–17]. Besides, current researches predominantly focus on inducing collagen regeneration while overlooking the role of other tissues in skin augmentation, such as blood vessels. Blood vessels play crucial role in

Peer review under responsibility of KeAi Communications Co., Ltd.

* Corresponding author. State Key Laboratory of High Performance Ceramics and Superfine Microstructure, Shanghai Institute of Ceramics, Chinese Academy of Sciences, 1295 Dingxi Road, Shanghai, 200050, PR China.

** Corresponding author. State Key Laboratory of High Performance Ceramics and Superfine Microstructure, Shanghai Institute of Ceramics, Chinese Academy of Sciences, 1295 Dingxi Road, Shanghai, 200050, PR China.

*E-mail addresses:* zhuyufang@mail.sic.ac.cn, zjf2412@163.com (Y. Zhu), chengtiewu@mail.sic.ac.cn (C. Wu).

[1] These authors contributed equally to this work.

https://doi.org/10.1016/j.bioactmat.2024.10.014
Received 16 July 2024; Received in revised form 30 September 2024; Accepted 16 October 2024
2452-199X/© 2024 The Authors. Publishing services by Elsevier B.V. on behalf of KeAi Communications Co. Ltd. This is an open access article under the CC BY-NC-ND license (http://creativecommons.org/licenses/by-nc-nd/4.0/).

transporting oxygen and nutrients while eliminating waste products [18]. Thus, they are considered beneficial for facilitating tissue regeneration [19]. To the best of our knowledge, there was few soft tissue fillers have been reported to have the abilities of vascularization and collagen regeneration [20].

In the past decades, silicate bioceramics have been demonstrated remarkable excellent physiological functions in hard and soft tissue regeneration due to the released bioactive ions [21–23]. Silicate (Si) ion has exhibited positive effect on the collagen secretion by activating the EMT and EndMT signaling pathways [24]. Several studies have demonstrated that the extracts of silicate bioceramics could initiate the proangiogenesis [25–27].Our previous studies found that silicate bioceramics could promote the regeneration of collagen and blood vessels in skin tissue [24,28–30]. On the other hand, lithium (Li) ions could act to induce proangiogenic and vascularization by eliciting the expression of exosomes [31]. In addition, the degradation of silicate bioceramics also avoided the risk of long-term implantation. Considering the biological functions of Si and Li ions, lithium calcium silicate bioceramics may have significant potential in skin augmentation as soft tissue fillers.

For the added component of tissue-induced fillers, it is usually select microsphere particles instead of irregular particles. Microspheres possess better homogeneity of shape and smooth surface, which favors injection and avoids tissue damage from the sharp surfaces of irregular particles. Moreover, small nanoscale size microspheres may enter blood vessels, potentially leading to capillary embolism and subsequent tissue necrosis [32]. Besides, small size microspheres were more easily taken up by macrophage and lose their function. Conversely, the large particles may also result in perceptible granularity and discomfort among users. Currently, the majority of commercial products contain microspheres ranging in size from 20 to 50 μm. However, conventional synthesis methods, such as sol-gel, microemulsion and flame spheroidization, are difficult to achieve large-scale production of silicate ceramic microspheres with complex compositions and uniform shapes at low cost [33,34].

In this study, a simple and cost-effective sol-spray route was successfully proposed to synthesize lithium calcium silicate ($Li_2Ca_4Si_4O_{13}$, LCS) bioceramic microspheres with average diameter of 25.6 μm. The injectable HA-LCS bioactive skin tissue fillers were prepared by incorporating LCS microspheres into HA hydrogel (see Scheme 1). The incorporation of these microspheres as bioactive ingredients endowed the fillers with excellent biological properties. In detail, the cytocompatibility, collagen promotion, and vascularization activities *in vitro* of HA-LCS fillers were assessed through cell experiments including cytotoxicity evaluation, cell proliferation analysis, and gene expression profiling. Furthermore, successful collagen and vascular regeneration were observed upon injection into mouse skin tissues. Overall, these injectable fillers containing silicate bioceramic microspheres have great potential as next-generation skin tissue fillers.

## 2. Materials and methods

### 2.1. Materials

Calcium nitrate tetrahydrate ($Ca(NO_3)_2{\cdot}4H_2O$), lithium nitrate ($LiNO_3$), hyaluronic acid (HA) and 1,4-butanediol diglycidyl ether (BDDE) were purchased from Shanghai Aladdin Biochemical Technology Co., Ltd (China). Sodium hydroxide (NaOH) and nitric acid ($HNO_3$) were purchased from Sinopharm Chemical Reagent Co., Ltd. Ethyl silicate (TEOS) was purchased from Shanghai Lingfeng Chemical Reagent Co., Ltd.

### 2.2. Preparation of LCS microspheres

The LCS microspheres were prepared by a sol-spray method. Typically, 1 mol of TEOS was mixed with 8 mol of deionized water and 0.16 mol of $HNO_3$ under stirring until the solution become transparent. Subsequently, 1 mol of $Ca(NO_3)_2{\cdot}4H_2O$ and 0.5 mol of $LiNO_3$ were added into the mixed solution and stirred for 1 h. To prevent pipe clogging, the concentration of the solution was adjusted by adding deionized water. Then, the mixed slurries were transformed into gel microspheres by a spray granulator (Shanghai Qiaofeng Industrial Co., Ltd) with the predetermined parameters. The LCS bioceramic microspheres were fabricated after sintering at temperature of 940 °C for 3h (heating rate: 2 °C/min). Finally, small microspheres were removed using an 800 mesh sieve.

### 2.3. Preparation of HA-LCS tissue fillers

BDDE was selected as the crosslinking agent to prepare HA hydrogels. Briefly, HA powder was immersed in 1 wt% NaOH solution under mechanical stirring. After mixed with BDDE, the solution was crosslinked at the temperature of 50 °C for 4 h. To remove free BDDE and

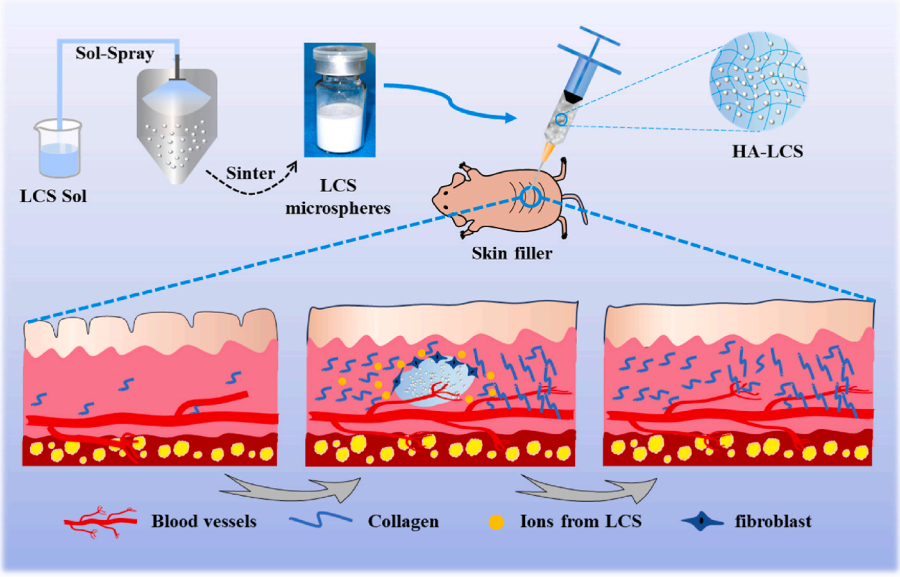


**Scheme 1.** Schematic illustration of the fabrication of HA-LCS fillers and its application for skin augmentation. The LCS microspheres were prepared by a sol-spraying method. These bioactive fillers exhibit the potential to stimulate collagen and blood vessel regeneration, thereby facilitating skin augmentation.

regulate osmotic pressure, the hydrogel was dialyzed in PBS for 24 h. Finally, HA hydrogel was obtained by adjusting mass fraction to 2 % using PBS. Different hydrogels were prepared by varying the addition of BDDE.

To prepare sterile fillers, the obtained HA hydrogel and LCS microspheres were sterilized at 121 °C in a sterilizer. Then, HA-LCS fillers were prepared by mixing hydrogel with LCS microspheres under mechanical stirring. A series of HA-LCS fillers containing 5, 10, 20 and 30 wt% LCS were prepared and named as HA-5LCS, HA-10LCS, HA-20LCS and HA-30LCS, respectively.

### 2.4. Characterization of materials

The microstructure and elemental mapping of materials was observed by the scanning electron microscopy (SEM, SU8220, SU9000, Japan). X-ray diffraction (XRD, D8 ADVANCE, Germany) was used to analyze the component of microspheres. The rheological properties of fillers were tested by Rheometers (MCR301, Austria). The heavy metal content was determined by inductively coupled plasma-mass spectrometry (ICP-MS, NexION 2000s, America) after dissolved LCS by HF solution. The Li and Si ions concentration of solution was measured by inductive coupled plasma atomic emission spectrometry (ICP-AES, Varian 715-ES, America).

### 2.5. Injection force testing

The injection force was determined using a standard mechanical testing machine (UTM4304X, China). The fillers were added into 1 mL syringes with 27 G needle and placed inside a sleeve (Fig. 2d). The average injection force and displacement-force curve were measured at a loading speed of 30 mm/min.

### 2.6. Water absorption

The fillers were injected into a mold and put into fridge at −80 °C. After freeze drying, the dry weight of fillers was determined by analytical balance. Next, the dry fillers were soaked into PBS for 24 h and then measured the wet weight. The water absorption was calculated by the equation:

$$\textbf{\textit{Water absorption}} = W_1/W_2 \times 100\%$$

where $W_1$ refers to the weight of the fillers after water absorption, $W_2$ refers to the dry weight of fillers before water absorption.

### 2.7. Degradation in vitro

The freeze-drying samples were immersed into 5 mL Tris-HCl buffer. The weight was measured at each predetermined time point after freeze drying. The degradation rate of fillers with different content of LCS microspheres were determined after soaking for 7, 14 and 28 days.

### 2.8. Ions release of microspheres and fillers

The LCS microspheres and HA-LCS fillers were soaked in serum-free DMEM (Dulbecco's Modified Eagle Medium) to explore the release of ions. Typically, 70 mg of LCS microspheres or 0.2 mL of fillers was soaked in 5 mL of DMEM for 1, 4, 7 and 14 days. The solution was put in a shaker at the temperature of 37 °C and the shaking frequency of 100 rpm. The concentration of released ions was measured by inductive coupled plasma atomic emission spectrometry (ICP-AES, Varian 715-ES, America).

### 2.9. In vitro cytocompatibility

*Cell culture.* To evaluate cytocompatibility of LCS microspheres, the extracts were prepared by incubating microspheres into serum-free DMEM or ECM at a concentration of 50 mg/mL in a shaker for 24 h to culture cells. After sterilization through filtration, DMEM or ECM was added into extracts to prepare serial dilutions of extracts (1/2, 1/4, 1/8, 1/16, 1/32, 1/64, 1/128 and 1/256). For HA-LCS fillers, the extracts were replaced by transwell inserts (NEST Biotechnology) with 50 μL HA-LCS fillers. Human dermal fibroblasts (HDFs) and human umbilical vein endothelial cells (HUVECs), obtaining from Cyagen Biosciences, were cultured with DMEM and Endothelial Cell Medium (ECM) with serum and antibiotics at 37 °C in a humidified $CO_2$ incubator, respectively. The medium was refreshed daily.

*Cytotoxicity assay.* To evaluate cytotoxicity of LCS microspheres, the cells (HDFs or HUVECs, $5.0 \times 10^4$ cells per well) were seeded in the 24-well culture plates with extracts for 24 h. Subsequently, the cells were incubated with 10 % CCK8 medium (Dojindo, Japan) for 2 h, and then followed by measurement of absorbance at 450 nm using a microplate reader (Spark, Tecan, Switzerland). The same methodology was employed to evaluate the cytotoxicity of fillers.

*Live and dead staining.* The live/dead assay was performed to evaluate the viability of HDFs and HUVECs according to the manufacturer's instruction. Briefly, a staining solution was prepared by diluting the Calcein-AM/PI staining kit (Dojindo, Japan) with PBS in a volume ratio of PBS: AM: PI = 100: 2: 3. After 24 h of culturing, cells were incubated with the staining solution at 37 °C for 10 min. The fluorescence microscope (DMi8 S, Leica, Germany) was used to observe the constructs. Dead cells were stained in red and live cells were stained in green with lights at wavelengths of 556 nm and 448 nm, respectively.

*Cell morphology.* To visualize the cell morphology, cells cultured for 3 days were fixed with 4 % paraformaldehyde for 30 min. Following triple washing with PBS, the cytoskeleton was labeled using Alex Fluor 488-conjugated phalloidin (Molecular Probes, USA), while the cell nucleus was stained with Diamidinophenylindole (DAPI, Sigma-Aldrich). Subsequently, confocal images were obtained by confocal laser scanning microscopy (CLSM, TCS SP8, Leica, Germany) to observe cell morphology.

*Cell proliferation.* For the cell proliferation, the culture time were 1, 3 and 7 days with the initial cell density of 5000 cells per well. The cell proliferation of the extracts and fillers were determined by the same methods with cytotoxicity assay. The absorbance of medium at various time points were measured by microplate reader at 450 nm.

### 2.10. Gene expression analysis

To investigate the impact of HA-LCS fillers on the expression of collagen-related genes, HDFs were cultured for 5 days and subsequently treated with Trizol Reagent (Invitrogen Pty Ltd, Australia) to extract total RNA. Subsequently, cDNA was obtained by using PrimeScript 1st Strand cDNA synthesis kit (TOYOBO, JAPAN). Finally, the real-time quantitative polymerase chain reaction (RT-qPCR) process was conducted by StepOnePlus Real time systems (Applied Biosystems, USA). The housekeeping gene GAPDH was used to normalize the results by the $2^{-\Delta\Delta CT}$ method. A similar protocol was employed to assess the effect of HA-LCS filler on angiogenesis-related gene expression in HUVECs. The sequences of primers for the above genes were shown in Supplementary Table S3.

### 2.11. Immunofluorescence protein staining

The relative protein expression level was assessed by immunofluorescence staining assay. Briefly, the cells were firstly cultured with fillers for 5 days and then fixed in 4 % paraformaldehyde. Subsequently, 5 % BSA solution were used to block the samples to avoid non-specific bindings. After that, primary antibodies were added at 4 °C for more than 12 h and then followed by washing with PBS. Finally, the samples were immersed into secondary antibody solution for 1 h. After washing with PBS for 3 times, the cell nuclei and cytoskeleton were stained by

DAPI and FITC solution. Finally, the images were obtained under CLSM.

### 2.12. Tube formation assay

200 μL Matrigel (354262, Corning, USA) were added into culture well after thawing at 4 °C. Following incubated in the incubator for 1 h, HUVECs were seeded on Matrigel (354262, Corning, USA). The fillers were placed in the transwell and then co-cultured for 6 h. Then, the tube formation status of HUVECs in each group was recorded by microscope. The number of junctions and meshes in each field were further analyzed by Image J software.

### 2.13. In vivo collagen secretion and vascular regeneration

All animal experiments were performed in accordance with the guidelines approved by the Institutional Animal Care and Use Committee of Nanjing First Hospital, Nanjing Medical University (DWSY-22030156). To evaluate the impact of the injectable HA-LCS filler on collagen and vascular regeneration, the BALB/c nude mice (female, 5 weeks old) model with skin wrinkling was established using 1α,25-dihydroxyvitamin $D_3$ ($1,25(OH)_2VD_3$, $VD_3$) for 3 weeks as previously reported [35,36]. Following treatment, 200 μL of fillers were injected into the dorsal skin of mice. The mice were divided into six groups: Blank (untreated and unfilled), Control (treated but unfilled), HA, HA-5LCS, HA-10LCS and HA-20LCS. After 8 weeks, the mice were sacrificed. The skin samples at the filling area were harvest and fixed in 4 % paraformaldehyde solution for further analysis. To determine the long-term degradation *in vivo* of HA-LCS filler, the same animal experiment was conducted to obtain optical pictures after injection for 5 months.

For quantitative analysis of collagen secretion of fillers, a HYP Content Assay Kit (Sangon Biotech, China) was used to measure the collagen content of the skin tissues. Furthermore, the samples were incubated in PBS solution with 10 % sucrose for 4 h and transferred into PBS solution with 30 % sucrose for 2 days. Then, the samples were embedded and sectioned into histological slices by using Frozen Slicer (NX70, epredia, America). H&E staining (C0105S, Beyotime, China) was conducted to observe skin tissue around filling area for histology analysis. Masson staining was used to evaluate the amount of collagen production at the filling area.

In addition, to observe the morphology of LCS microspheres in the tissue, the skin tissues were sectioned into 50 μm thickness. Then, the samples were processed with 2.5 % glutaraldehyde for 1 h at 4 °C and gradient ethanol solution (50 %, 70 %, 80 %, 90 %, 100 %). After drying at room temperature, the samples were observed by SEM.

To further evaluate the collagen and vascular regeneration, immunofluorescence staining was performed as follows. Firstly, the frozen slices were thawed at room temperature for 4 h and washed with PBS. Then, the slices were incubated with ultrapure water with 5 % 1 M Tris-HCl (pH = 8.0), 1 % 0.5 M EDTA and 0.06 % 20 mg/mL proteinase K at 37 °C for 15 min to repair antigen. Subsequently, the slices were blocked by PBS/10 % horse serum with 0.3 % Triton X-100 for 1 h. After incubated with primary antibodies overnight at 4 °C, the slices were incubated with fluorescent secondary antibody for 1 h at room temperature under light protection. Finally, the stained slices were mounted by Antifade Mounting Medium with DAPI (BL739B, biosharp, China) and photographed by confocal laser scanning microscopy (TCS SP8, Leica, Germany). The semi-quantitative analyses were processed by the Image J software.

### 2.14. In vivo biosafety assessment

To evaluate the biocompatibility of HA-LCS fillers, 200 μL fillers were injected into dorsal skin of white mice (female, 5 weeks old) for 3 and 7 days. The tissues at filling site were harvested and sliced for H&E staining and immunofluorescence staining of relevant inflammatory markers.

To further evaluate the biosafety of HA-LCS fillers, the visceral tissue (heart, liver, spleen, lungs and kidneys) was harvested after inject for 2 weeks and fixed in 4 % paraformaldehyde solution. Subsequently, they were soaked in PBS solution containing 10 % sucrose for 4 h followed by PBS solution with 30 % sucrose for 2 days. After sliced, the tissues were performed by H&E staining to assess biosafety of fillers. In addition, the complete blood count (CBC) analysis and H&E staining of subcutaneous tissue were conducted to prove long-term safety and inflammatory response of HA-LCS fillers after injection for 4 weeks.

### 2.15. Statistical analysis

All data were shown as mean ± standard deviation (SD). Significant differences were determined with student's t-test. A P-value <0.05 was considered significance difference (*$p < 0.05$, **$p < 0.01$, ***$p < 0.001$).

## 3. Result and discussion

### 3.1. Preparation and characterization of LCS microspheres

In this study, the LCS bioceramic microspheres were successfully prepared through a sol-spary route by combining sol-gel and spray granulation method. SEM images demonstrated the excellent sphericity of the LCS ceramic microspheres with an average particle size of 25.6 μm (Fig. 1a and b and Fig. S1a). The elemental mapping of microspheres showed that the elements uniformly distributed in the microspheres (Fig. S2). XRD analysis confirmed that the phase of microspheres was $Li_2Ca_4Si_4O_{13}$ (PDF#82–1106) (Fig. 1c). The degradation experiment revealed an increase in Li ion concentration over time in soaking solution of LCS, reaching a concentration of 158 ppm after 14 days of immersion (Fig. S1b). To determined relative content of LCS microspheres, the microspheres was dissolved in HF solution. Then, the ions concentration of Li, Ca and Si was determined by ICP analysis. The ions concentration was 0.023 mg/L, 0.274 mg/L and 0.178 mg/L. The calculated mass ration was 1:11.91:7.74 (Li: Ca: Si), which is similar to the theoretical mass ratio (1: 11.55: 8.09) (Table S1). The concentrations of several heavy metals (Cr, As, Cd, Hg and Pb) were found to be below 0.05 mg/kg, which could satisfy with the requirements for medical devices (Table S2).

### 3.2. Preparation and characterization of HA-LCS filler

Hyaluronic acid (HA), the main component in dermal skin, played crucial physiological roles on water retention, lubrication, skin augmentation and so on [37]. Owing to its exceptional biocompatibility, it had been extensively employed as a dermal filler for several decades. However, the multi-injection was needed due to its fast degradation rate and poor support. In this study, different amounts of BDDE, *i. e.*67, 100 and 200 mg/g ($m_{BDDE}/m_{HA\ powder}$), were used to cross-link HA in order to enhance its durability. The $^1H$ NMR results revealed that HA hydrogels exhibited higher degrees of crosslinking with increasing amounts of BDDE (Fig. S3a). Furthermore, the absorbance curve of HA degradation products showed that the HA hydrogels were more difficult to degrade under enzymatic catalysis with the increase content of BDDE (Fig. S3b). Additionally, the viscosity and injectable force of HA hydrogels also increased with the addition of BDDE (Fig. 2e, Fig S3c and Fig. S4). Therefore, considering injectability and degradability factors for subsequent experiments, a final amount of 100 mg/g (BDDE/HA powder) was selected.

The HA-LCS tissue fillers were prepared by mixing HA hydrogel with LCS microspheres under mechanical stirring. To investigate the effect of different ceramic microspheres contents on fillers, LCS microspheres were added into HA hydrogels to obtain four types of fillers that named as HA-5LCS (5 wt% LCS), HA-10LCS (10 wt% LCS), HA-20LCS (20 wt%

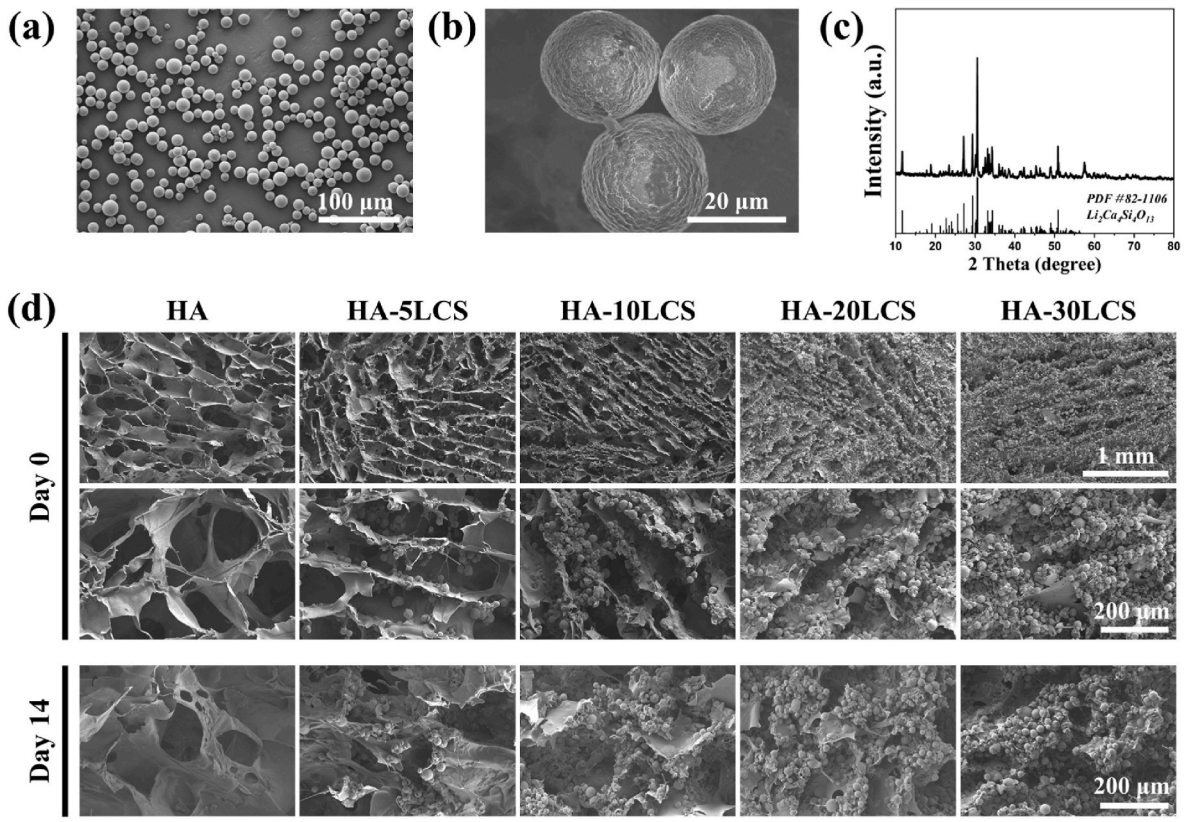


**Fig. 1.** The morphologies and composition of LCS microspheres and tissue fillers. SEM images (a, b) and XRD pattern (c) of prepared LCS microspheres. (d) SEM images of tissue fillers containing different ceramic before and after soaking in PBS for 14 days. The LCS microspheres were fabricated by a sol-spraying method and dispersed in HA hydrogel homogeneously.

LCS), and HA-30LCS (30 wt% LCS), respectively. Subsequently, the SEM images revealed that LCS microspheres dispersed in hydrogel uniformly after freeze drying (Fig. 1d). Furthermore, the rheological tests were carried out to evaluate the variations in storage modulus (G′) and loss modulus (G″) and complex viscosity of HA-LCS fillers. As shown in Fig. 2a and b, the value of G′ and G″ were significantly increased due to the addition of LCS microspheres. Furthermore, for all of HA-LCS fillers, the value of G′ was always higher than that of G″ in the frequency of 0.01–100 Hz, indicating the elastic solid properties of HA-LCS fillers. Furthermore, although the complex viscosity of fillers increased with the increase of LCS microspheres content, it was observed that the addition of LCS microspheres did not affect the shear thinning property of fillers. This shear thinning property facilitated the injectability of HA-LCS fillers, which was indispensable for non-invasive operation. Typically, a better injectability means that fillers could be injected through tinier needle to minimize wounds.

To further evaluate the injectability of fillers, a simple system with 27 G needle was prepared to test the injection force (Fig. 2d). The injection force increased with the increase of microspheres content, which corresponds to the change of complex viscosity (Fig. 2e). However, the average injection force of all HA-LCS fillers was lower than 36 N, indicating that these fillers can be easily administered manually by medical practitioners. Additionally, the displacement-load curve illustrated that the injection force of HA-LCS fillers exhibited minimal fluctuations within a narrow range, highlighting the homogeneity of fillers (Fig. 2f). Stable and low injection forces were fundamental properties for clinical application of these fillers. Consequently, HA-LCS fillers possessed characteristics that were practitioner-friendly and patient-friendly due to their good injectability. In addition, the water absorption ratio of fillers decreased significantly with the increase of microspheres content, indicating the better stability of filler *in vivo* (Fig. 2g and S5).

The concentration of Li and Si ions released from fillers were also determined by ICP analysis. It was easy to observe that the ions concentration raised with the increase of LCS content, while the release rate slowed down with soaking time (Fig. 2h and i). Meanwhile, the degradation rate of HA-LCS fillers increased with the increase of LCS microspheres content and decreased with increasing soaking time (Fig. S6). After soaking for 14 days, the Li ions concentration of HA-5LCS reached about 51.9 ppm while the Li ion concentration of HA-30LCS reached about 342.1 ppm. As for Si ions, the ion concentration of HA-5LCS, HA-10LCS, HA-20LCS and HA-30LCS was 180.5, 189.9, 219.5 and 240.7 ppm at day 14, respectively. Additionally, SEM images showed no significant changes in filler structure after soaked in PBS for 14 days (Fig. 1d). Several studies had demonstrated that the released bioactive ions with appropriate concentration possessed excellent biological effect on cells fate while excessive ions concentration had negative influence [38,39]. Therefore, the proper content of LCS microspheres in fillers was further investigated through biological experiments.

### 3.3. *In vitro* biological properties of LCS microspheres and HA-LCS fillers

The cytotoxicity, cell proliferation and live/dead staining were conducted to determine the *in vitro* biological properties of LCS microspheres extracts. HDFs and HUVECs were cultured with various concentration extracts. The cell viability assays showed that the extracts did no exhibit significant cytotoxicity towards HUVECs at extract concentrations lower than 1/32 and HDFs at extract concentrations lower than 1/4, by the fact that cells viabilities were more than 90 % compare with blank group (Fig. 3a and c) [40]. Furthermore, live-dead staining images revealed that cells cultured with 1/128 and 1/64 dilutions for HUVECs and HDFs exhibited good survival rates respectively (green points), while a high concentration of extract (1/2 dilutions) resulted in extensive cell death (red points) (Fig. 3e). The above results revealed that the excessive concentration of LCS extracts led to the reduction of biological

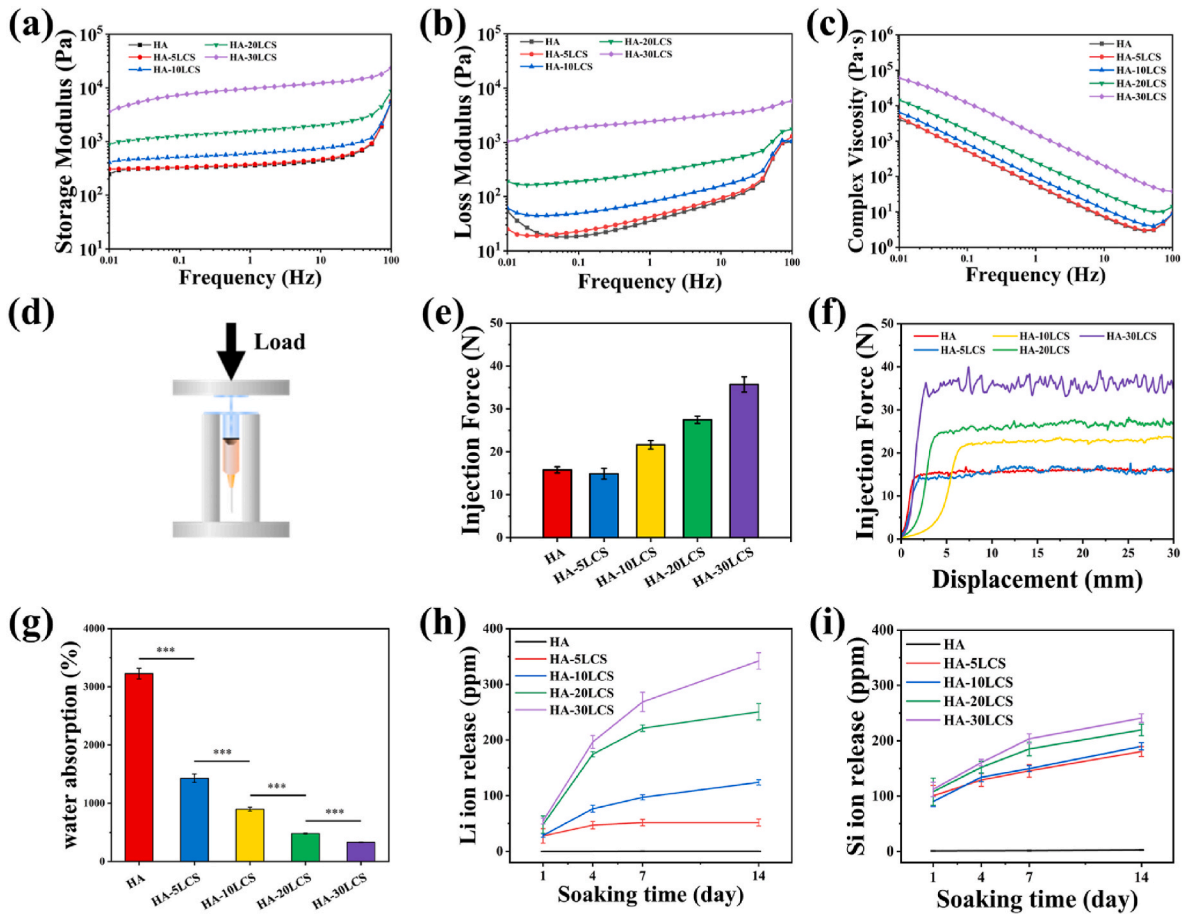


**Fig. 2.** Characterization of physicochemical properties of tissue fillers. (a, b, c) Rheological properties of tissue filler at the frequency ranging from 0.01 to 100 Hz. (d) Schematic illustration of the injection force measurement. The average injection force (n = 5) (e) and displacement-load curve (f) of tissue fillers at the speed of 30 mm/min. (g) The water absorption ratio of tissue fillers (n = 5). (h, i) The change of ions concentration of samples after soaking with DMEM. The fillers exhibited properties of shear thinning, injectability and ions release (n = 5).

proprieties, which could be attributed to the high concentration of ions and high pH value. Subsequent cell proliferation assays showed favorable effects on HUVECs at the extract concentrations below 1/32 and on HDF at extract concentrations below 1/16, respectively (Fig. 3b and d). Therefore, careful consideration should be given to the amount of LCS used in preparing HA-LCS fillers with optimal biological properties.

Furthermore, the *in vitro* biological properties of HA-LCS fillers were also investigated. HA-LCS fillers were added into transwell inserts to culture cells (Fig. 4a). The cell proliferation assays of HUVECs demonstrated that the HA-5LCS and HA-10LCS fillers had no obvious influence on cell proliferation, while HA-20LCS and HA-30LCS groups exhibited slightly negative influence (Fig. 4b). As for HDFs, only HA-30LCS group exhibited a negative effect on cell proliferation (Fig. 4c). Live/dead staining images revealed an abundance of dead cells in the HA-30LCS group (Fig. 4d). In addition, immunofluorescence images revealed that cells in HA-30LCS group displayed poor morphology compared to other groups (Fig. 4e). The negative effect of HA-30LCS filler on cells could be attributed to the rapid increase in pH value and ion concentration caused by excessive LCS microsphere content. Therefore, the gene expression assays of HA-30LCS filler were not carried out in later due to its poor cytocompatibility.

The abilities of HA-LCS fillers to regulate gene expression on vascularization and collagen secretion were also assessed by qPCR. The expression of VEGF, bFGF and HIF-1α was determined to evaluate the effect of HA-LCS fillers on angiogenesis *in vitro*. Compared to the blank group, all groups treated with HA-LCS fillers (HA-5LCS, HA-10LCS and HA-20LCS) could enhance the expression of VEGF and bFGF (Fig. 4f and S8a). For HIF-1α, HA-5LCS exhibited highest expression level (Fig. S8b). The CD31 protein expression and tubule experiments were conducted to further assess the ability of vascularization of HA-LCS. The CD31 protein expression level of HA-LCS groups was significantly higher than those of blank and HA groups, suggesting that LCS microspheres could promote vascularization (Fig. S9). In addition, the tube formation experiment results confirmed that the number of junctions and meshes in HA-LCS groups were obviously higher than other groups, among which HA-10LCS exhibited best capacity to promote tube formation (Fig. S10). Similarly, a positive effect was observed for collagen-related genes, specifically COL I for the HA-5LCS and HA-10LCS filler groups, as well as COL III for all groups (Fig. 4g and h). The results confirmed that HA-LCS fillers possessed favorable biological properties regarding the regulation of VEGF, COL I, and COL III gene expressions.

### 3.4. *In vivo* collagen regeneration and vascularization

Encouraged by the promoting effect of HA-LCS fillers on angiogenesis and collagen secretion-related genes expressions *in vitro*, we further evaluated their potential for vascularization and collagen regeneration *in vivo*. The nude mice with wrinkled and collagen-damaged skin were used as the animal model to evaluate the *in vivo* biological performance. The mice of blank group were untreated with $VD_3$ to induce the wrinkled and collagen-damaged skin. The mice of control group were treated $VD_3$ but not injected with fillers. For the groups of HA and HA-LCS, 200 μL of fillers were injected into the subcutaneous tissue of nude mice. It is observed that HA-LCS fillers provided continuous support for skin

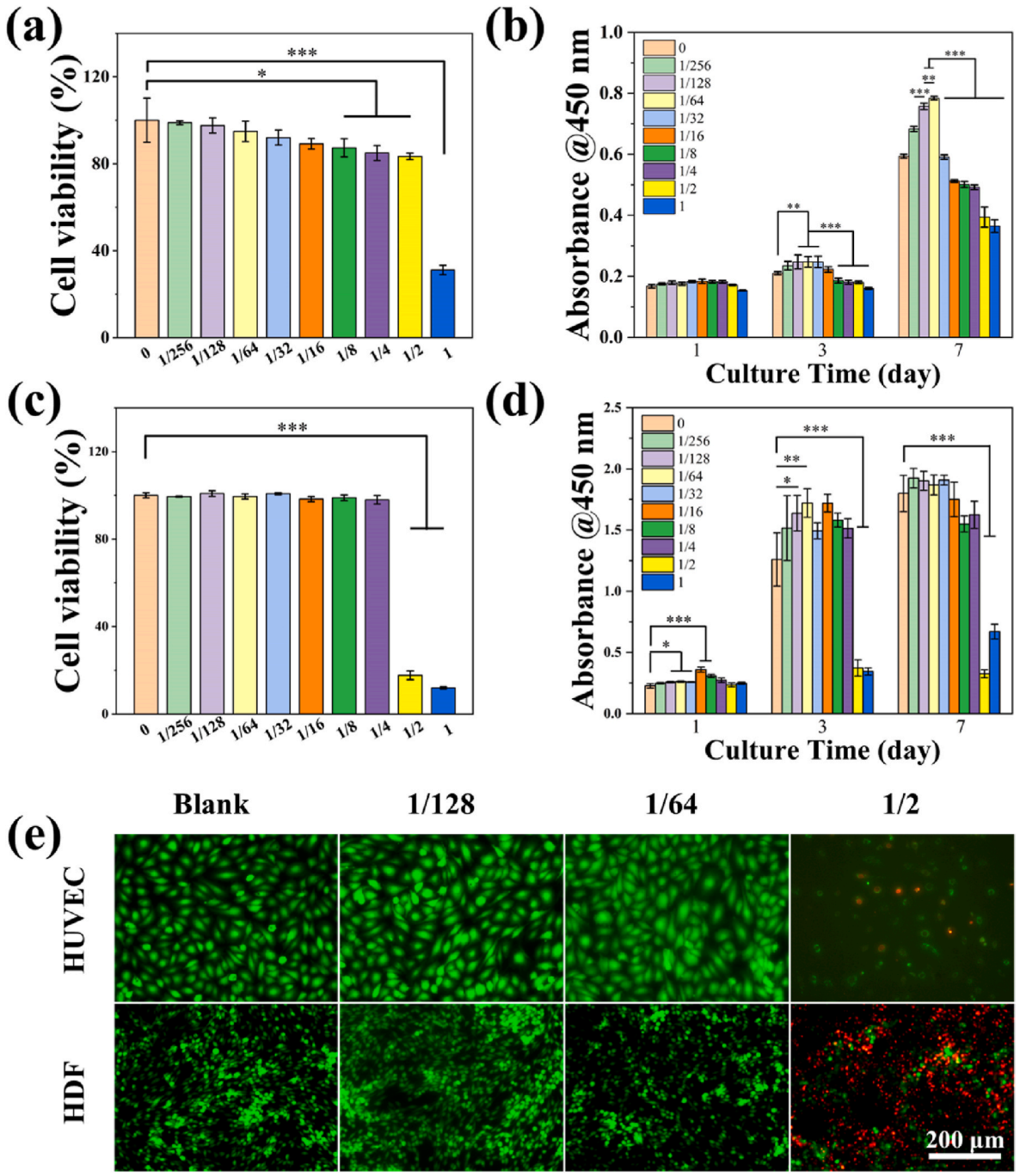


**Fig. 3.** The biological properties of LCS ceramic microspheres. Cell viability for 24 h and cell proliferation of HUVECs (a, b)and HDFs(c, d) (n = 7). (e) Live-dead staining of cells after cultured for 24 h. The results indicated excessive LCS microspheres could induce cell necrosis.

augmentation for at least 8 weeks. On the contrary, the pure HAfillers were almost degraded completely and lost the supporting effect at 4 weeks in HAgroup (Fig. 5b). Furthermore, HA-10LCS and HA-20LCS groups showed little wrinkled skin and better supporting effect than other groups (Fig. 5b and d). In addition, the *in vivo* degradation of HA-10LCS fillers after 8 weeks of injection were also investigated. There were many incomplete degraded HA-LCS fillers in subcutaneous tissue from histological images and SEM images at injection site, avoiding the rapid degradation issue of HA (Fig. 5d and e and S12). In addition, after injection of 8 weeks, none of dense collagen tissues were formed in injection sites similar to the collagen in newly bone (Fig. 5d), indicating that the HA-LCS fillers possessed less potential risk to promote bone tissue regeneration [41]. All of results indicated that the addition of LCS microspheres facilitated the long-term supporting effect of HA-LCS fillers.

Blood vessels, the conduits for transporting nutrients, played a pivotal role for growth and secretion of tissue [42]. It could be observed in optical photographs that higher presence of mature blood vessels in the skin tissue of the HA-LCS fillers groups than control and HA groups (Fig. 5b). Particularly, as a marker of vascular endothelial cells, CD31 played a significant role in vascularization [43,44]. Therefore, the expression of CD31 was also detected to evaluate the vascularization ability of HA-LCS fillers. The immunofluorescence staining images and semi-quantitative analysis confirmed that HA-10LCS fillers significantly promoted blood vessel growth and possessed the highest CD31 density comparing with HA fillers (Fig. 6a and b). These results demonstrated

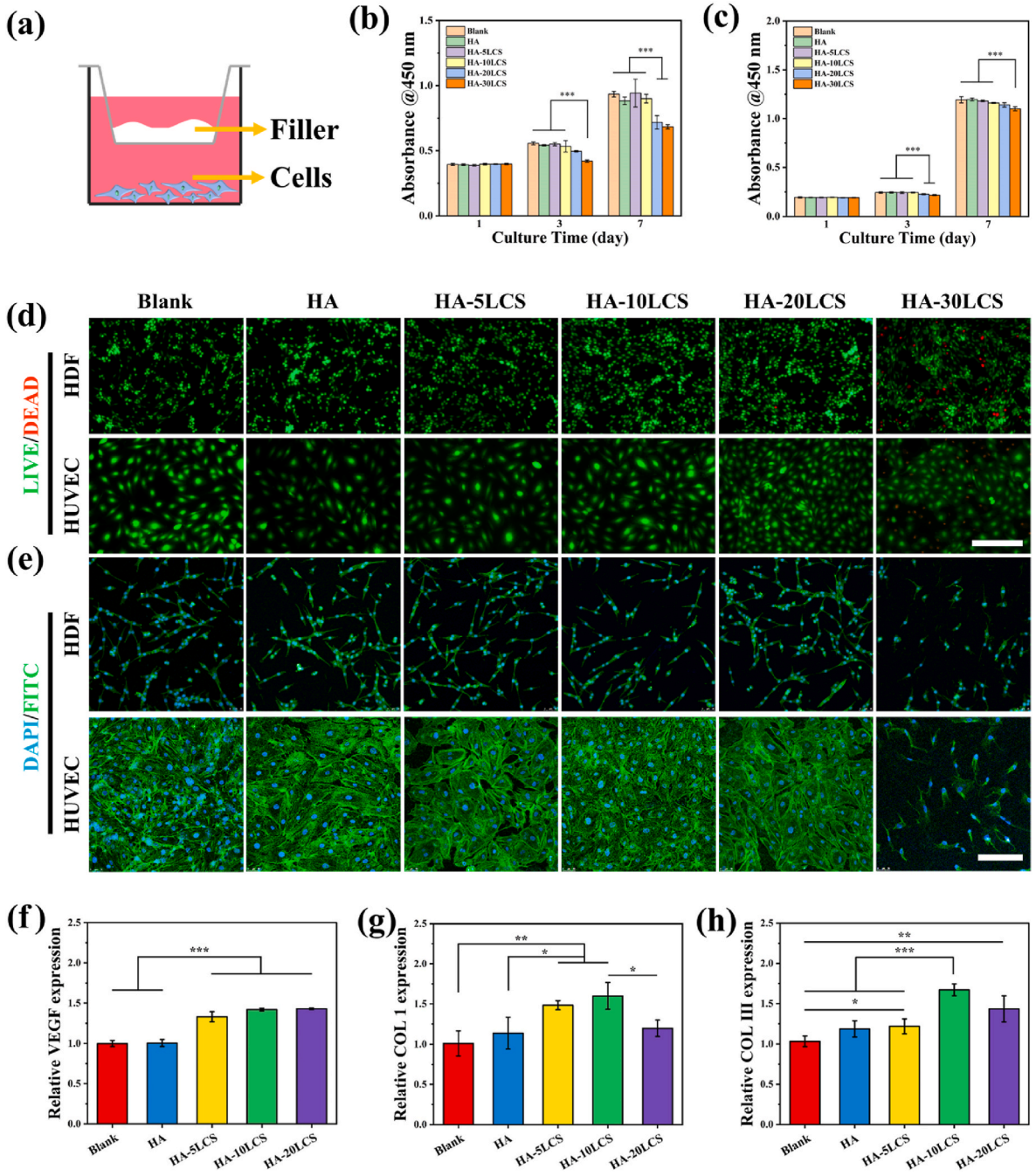


**Fig. 4.** The biological properties of tissue fillers. (a) The schematic illustration of cells culture. Cell proliferation of HUVECs (b) and HDFs (c) cultured with tissue fillers (n = 7). (d) Live-dead staining of cells after cultured for 24 h (Scale bar: 200 μm). (e) Confocal images of cells cultured for 3days (Scale bar: 400 μm). (f–h) The Relative gene expression of cells cultured with tissue fillers for 5 days (n = 6). The fillers exhibited good cytocompatibility and displayed a beneficial effect on the expression of vascularization and collagen genic-related genes.

that LCS bioceramic microspheres in the fillers played the main effect on the promotion of blood vessel growth, which could be attributed to the release of bioactive ions from LCS microspheres.

Furthermore, the collagen regeneration of HA-LCS fillers were also investigated. Hydroxyproline (HYP) is one of the main components of collagen in the body [45]. The collagen content of skin could be measured by determining the content of HYP. The assays demonstrated that the HYP content of HA-10LCS group was similar with the blank group and significantly higher than that of control group (Fig. 5c). Masson staining images also revealed that all HA-LCS groups exhibited much more collagen area (blue) comparing with blank, control and HA groups (Fig. 5d). Collagen I and III which are predominant types of collagens in skin tissue played crucial roles in facial augmentation. To further confirmed the ability of HA-LCS fillers on promoting collagen secretion, collagen I and collagen III were marked by fluorescence antibody. For dermis layer, the immunofluorescence staining images and the semi-quantitative analysis indicated that the collagen I content in HA-LCS groups almost reached the similar level to the normal skin of blank group (Fig. 6a and c). Moreover, there were more collagen III were observed in HA-5LCS and HA-10LCS groups. Semi-quantitative analysis also showed that among these groups, HA-5LCS and HA-10LCS exhibited superior promotion of collagen III (Fig. 6a and d). Furthermore, the collagen III in subcutaneous tissue was also labeled to evaluate the collagen secretion around the fillers. In contrast to the dermis layer, a

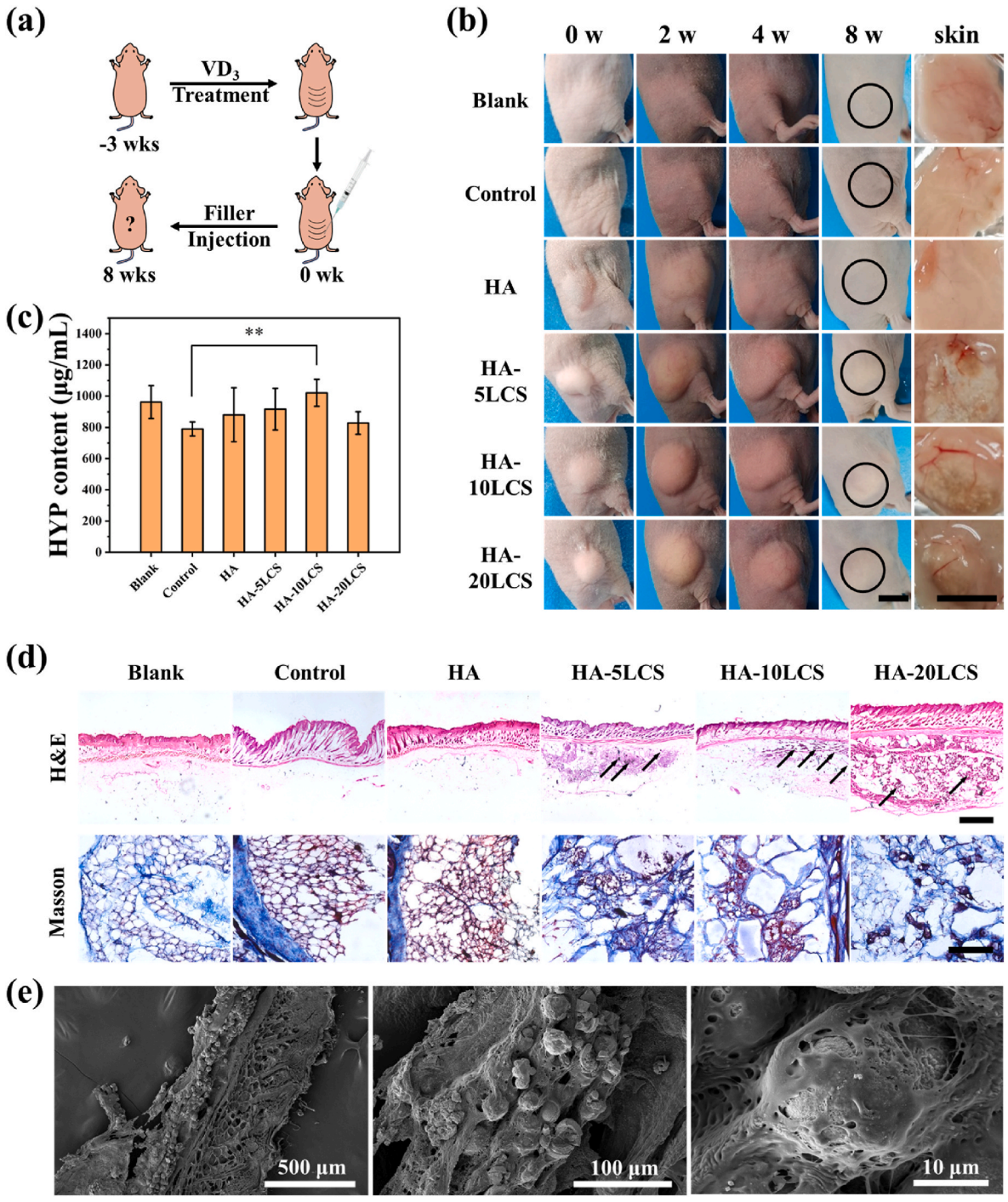


**Fig. 5.** In vivo collagen promotion and angiogenesis efficacy of tissue fillers. (a) Schematic illustration of the preparation of nude mice model and the effect after injection of tissue fillers. (b) The optical photos of mice after injection of tissue fillers at various time points (Scale bar: 1 cm). (c) The hydroxyproline content in skin tissues (n = 4). (d) H&E staining (scale bar: 1 mm; black arrows: the residual HA-LCS fillers) and Masson staining (scale bar: 400 μm) images of skin tissues at 8 weeks. (e) SEM images of tissue of HA-10LCS filler. The results demonstrated that tissue fillers exhibited a durable effect on tissue filling and effectively stimulated collagen synthesis and vascularization.

substantial amount of flexuous collagen III fibers was observed at the injection site (Fig. 6e). The ratio of collagen III to collagen I in fetal skin were higher than adult skin [46,47]. The content of collagen III decreased with the aging of skin, which led to the lack of elasticity of skin [48,49]. The silky fibers were similar to the results of Masson staining, suggesting that the HA-LCS fillers greatly promoted the secretion of collagen III (Fig. S11). Among all fillers, HA-10LCS exhibited superior efficacy in promoting subcutaneous tissue regeneration (Fig. 6f). Such remarkable ability of HA-10LCS fillers to regenerate collagen III would substantially contribute to rejuvenating aged skin.

Collectively, the HA-LCS fillers demonstrated a significant promotion in collagen secretion (collagen I and collagen III) within the dermal skin. Additionally, these fillers facilitated blood vessel growth and stimulated substantial secretion of collagen III in subcutaneous tissue. Considering the experimental results of HYP analysis and immunofluorescence staining, HA-10LCS exhibited optimal biological properties for vascular regeneration and collagen regeneration (as evidenced by total collagen content in both dermal skin and subcutaneous tissue according

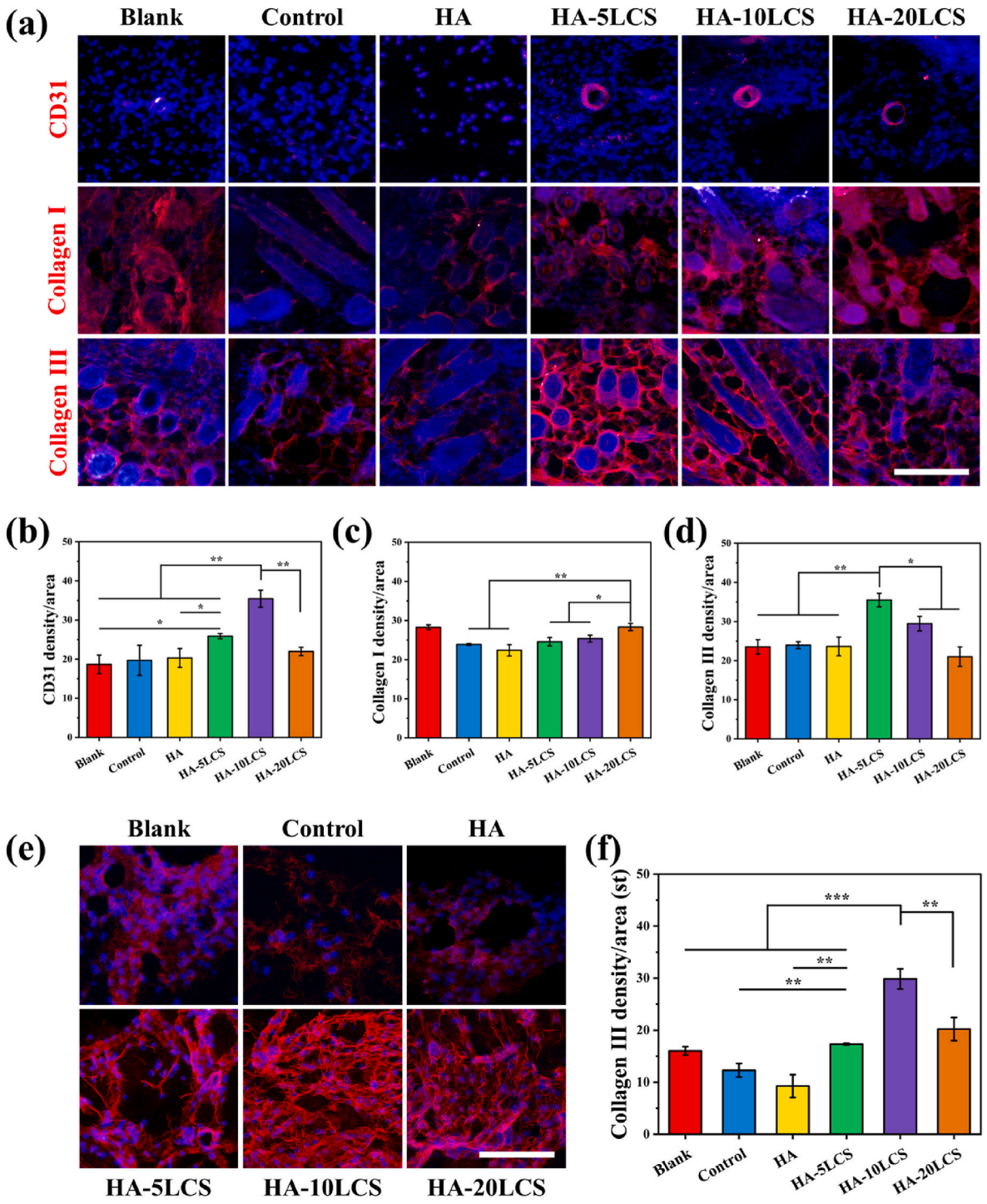


**Fig. 6.** Evaluation of the collagen secretion and vascularization of skin tissue after injection of fillers. (a) Representative immunofluorescence staining images of vascularization marker (CD31) and collagen markers (Collagen I and Collagen III in the dermis). (b–d) Semi-quantitative statistical analysis of all groups (n = 3). (e, d) Immunofluorescences staining images and semi-quantitative statistical analysis of Collagen III at the subcutaneous tissue (red) (n = 3). The prepared tissue fillers exhibited excellent abilities to promote collagen secretion and vascularization. (Scale bar: 200 μm).

to HYP assay results).

Furthermore, biosafety test plays a crucial role in evaluating the suitability of biomaterials. The *in vivo* biosafety experiment by mice subcutaneous implant model was conducted to assess biosafety of HA-10LCS filler. The H&E staining images of visceral tissue including heart, liver, spleen, lungs and kidneys showed that there were no obvious damage and inflammatory response (Fig. S13). In addition, although the H&E staining images of skin tissue exhibited the presence of several inflammatory cells after injected for 3 days, the inflammatory response significantly got better at day 7 (Fig. 7a). To further confirm biocompatibility of the filler, the inflammatory relevant markers, TNF-α and IL-6, were detected by immunofluorescence staining to further evaluate inflammatory response. The immunofluorescence images also revealed that a mild inflammatory response at day 3, but no obvious inflammatory response at day 7 (Fig. 7b and c). The acute inflammatory reactions were anticipated, but the prompt resolution of subsequent

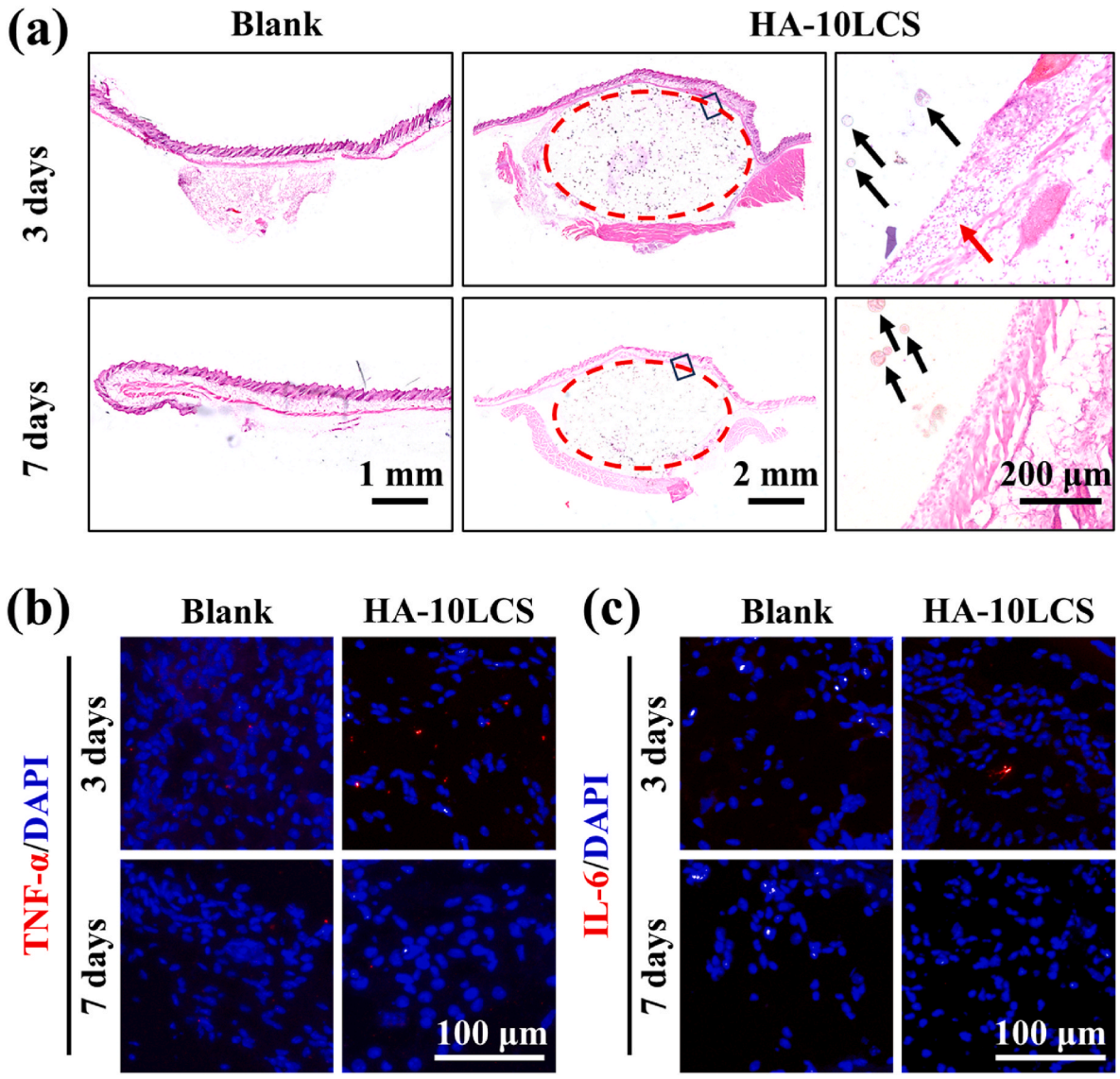


**Fig. 7.** Evaluation of inflammatory response after injection of HA-10LCS. (a) H&E staining images of skin tissues after injection (fillers were labeled by red circle. black arrow: LCS microspheres; red arrow: inflammatory cells). Immunofluorescence staining images of (b)TNF-α and (c) IL-6 at day 3 and day 7. HA-10LCS filler exhibited good biocompatibility and biosafety.

inflammatory responses also demonstrated the good biocompatibility of the filler. Furthermore, the long-term biosafety of HA-10LCS fillers was also investigated. After injection of fillers for 4 weeks, the complete blood count (CBC) analysis results showed that the number of different cells of HA-LCS group was similar to that of blank group without any fillers (Figs. S14a–g). In addition, the H&E staining images showed that there is no obvious macrophage and other inflammatory cells aggregation in HA-LCS group (Fig. S14h). Moreover, after injection of 5 months, the residue HA-LCS fillers greatly reduced comparing with initial fillers (Fig. S15). It was indicated that the HA-LCS fillers were gradually degraded with the regeneration of tissues, which would avoid chronic inflammation caused by prolonged presence of HA-LCS fillers. Therefore, the HA-LCS filler exhibited good biosafety and less risky of granuloma formation.

## 4. Conclusion

In summary, a sol-spray method was developed for the fabrication of LCS bioceramic microspheres, which were subsequently combined with HA hydrogel to prepare an injectable bioactive skin tissue filler. Such HA-LCS fillers not only avoided the fast degradation issue of HA or HA-based fillers, but also possessed outstanding advantages in promoting vascularization and collagen regeneration. The HA-10LCS fillers could stimulate the expression of angiogenesis-related and collagen-related genes. Moreover, *in vivo* evaluations further revealed that the HA-10LCS fillers promoted the secretion of collagen (collagen I and collagen III) in the dermis layer, as well as facilitated the production of collagen III fibers and blood vessel growth in the filled area. Additionally, mice subcutaneous implant models confirmed the biosafety of the fillers. To the best of our knowledge, this study represented the first report on the utilization of silicate bioactive ceramics for skin augmentation. Consequently, this injectable filler based on silicate bioceramic microspheres was considered as a promising filler for skin filling and was believed to possess enormous potential in promoting skin augmentation.

## CRediT authorship contribution statement

**Jinzhou Huang:** Writing – review & editing, Writing – original draft, Methodology, Investigation, Formal analysis, Data curation,

Conceptualization. **Jianmin Xue:** Writing – review & editing, Writing – original draft, Methodology, Investigation, Formal analysis, Data curation, Conceptualization. **Jimin Huang:** Formal analysis. **Xinxin Zhang:** Formal analysis. **Hongjian Zhang:** Methodology. **Lin Du:** Methodology. **Dong Zhai:** Methodology. **Zhiguang Huan:** Writing – review & editing, Data curation. **Yufang Zhu:** Writing – review & editing, Supervision, Resources, Funding acquisition, Conceptualization. **Chengtie Wu:** Writing – review & editing, Supervision, Resources, Funding acquisition, Conceptualization.

## Ethics approval and consent to participate

All animal experiments were performed in accordance with the guidelines approved by the Institutional Animal Care and Use Committee of Nanjing First Hospital, Nanjing Medical University (DWSY-22030156).

## Declaration of competing interest

Chengtie Wu is an editorial board member for *Bioactive Materials* and was not involved in the editorial review or the decision to publish this article. All authors declare that there are no competing interests.

## Acknowledgements

This work was supported by the National Natural Science Foundation of China (32225028 and 32130062), Shanghai Pilot Program for Basic Research-Chinese Academy of Science, Shanghai Branch (JCYJ-SHFY-2022-003), and Hengdian Group.

## Appendix A. Supplementary data

Supplementary data to this article can be found online at https://doi.org/10.1016/j.bioactmat.2024.10.014.

## References

[1] L. Baumann, Skin ageing and its treatment, J. Pathol. 211 (2) (2007) 241–251, https://doi.org/10.1002/path.2098.
[2] F. Bonté, D. Girard, J.-C. Archambault, A. Desmoulière, Skin changes during ageing, Sub-Cell Biochem 91 (2019) 249–280, https://doi.org/10.1007/978-981-13-3681-2_10.
[3] S. von Buelow, D. von Heimburg, N. Pallua, Efficacy and safety of polyacrylamide hydrogel for facial soft-tissue augmentation, Plast. Reconstr. Surg. 116 (4) (2005) 1137–1146, https://doi.org/10.1097/01.prs.0000179349.14392.a4.
[4] S.-W. Shin, Y.-D. Jang, K.-W. Ko, E.Y. Kang, J.-H. Han, T.M. Bedair, I.-H. Kim, T. I. Son, W. Park, D.K. Han, PCL microspheres containing magnesium hydroxide for dermal filler with enhanced physicochemical and biological performances, J. Ind. Eng. Chem. 80 (2019) 854–861, https://doi.org/10.1016/j.jiec.2019.07.043.
[5] A.W. Robert, F.A. Gomes, M.P. Rode, M.M. da Silva, M.B. da Rocha Veleirinho, M. Maraschin, L. Hayashi, G.W. Calloni, M.A. Stimamiglio, The skin regeneration potential of a pro-angiogenic secretome from human skin-derived multipotent stromal cells, J. Tissue Eng. 10 (2019) 1–10, https://doi.org/10.1177/2041731419833391.
[6] A. Fakhari, C. Berkland, Applications and emerging trends of hyaluronic acid in tissue engineering, as a dermal filler and in osteoarthritis treatment, Acta Biomater. 9 (7) (2013) 7081–7092, https://doi.org/10.1016/j.actbio.2013.03.005.
[7] S.J. Falcone, R.A. Berg, Crosslinked hyaluronic acid dermal fillers: a comparison of rheological properties, J. Biomed. Mater. Res., Part A 87A (1) (2008) 264–271, https://doi.org/10.1002/jbm.a.31675.
[8] G.D. Monheit, K.M. Coleman, Hyaluronic acid fillers, Dermatol. Ther. 19 (3) (2006) 141–150, https://doi.org/10.1111/j.1529-8019.2006.00068.x.
[9] F.S. Brandt, A. Cazzaniga, Hyaluronic acid gel fillers in the management of facial aging, Clin. Interv. Aging 3 (1) (2008) 153–159, https://doi.org/10.2147/cia.s2135.
[10] J.A. Kadouch, Calcium hydroxylapatite: a review on safety and complications, J. Cosmet. Dermatol. 16 (2) (2017) 152–161, https://doi.org/10.1111/jocd.12326.
[11] D. Thioly-Bensoussan, Non-hyaluronic acid fillers, Clin. Dermatol. 26 (2) (2008) 160–176, https://doi.org/10.1016/j.clindermatol.2007.09.017.
[12] K.W. Broder, S.R. Cohen, An overview of permanent and semipermanent fillers, Plast. Reconstr. Surg. 118 (3) (2006) 7S–14S, https://doi.org/10.1097/01.prs.0000234900.26676.0b.
[13] P.F. Jacovella, Calcium hydroxylapatite facial filler (Radiesse (TM)): indications, technique, and results, Clin. Plast. Surg. 33 (4) (2006) 511, https://doi.org/10.1016/j.cps.2006.08.002.
[14] M. Alam, J. Havey, N. Pace, M. Pongprutthipan, S. Yoo, Large-particle calcium hydroxylapatite injection for correction of facial wrinkles and depressions, J. Am. Acad. Dermatol. 65 (1) (2011) 92–96, https://doi.org/10.1016/j.jaad.2010.12.018.
[15] S.S. Johl, R.A. Burgett, Dermal filler agents: a practical review, Curr. Opin. Ophthalmol. 17 (5) (2006) 471–479, https://doi.org/10.1097/01.icu.0000243021.20499.4b.
[16] G. Lemperle, N. Gauthier-Hazan, M. Wolters, M. Eisemann-Klein, U. Zimmermann, D.M. Duffy, Foreign body granulomas after all injectable dermal fillers: Part 1. Possible causes, Plast. Reconstr. Surg. 123 (6) (2009) 1842–1863, https://doi.org/10.1097/PRS.0b013e31818236d7.
[17] E. Skrzypek, B. Gornicka, D.M. Skrzypek, M.R. Krzysztof, Granuloma as a complication of polycaprolactone-based dermal filler injection: ultrasound and histopathology studies, J. Cosmet. Laser Ther. 21 (2) (2019) 65–68, https://doi.org/10.1080/14764172.2018.1461229.
[18] G. Li, Q. Han, P. Lu, L. Zhang, Y. Zhang, S. Chen, P. Zhang, L. Zhang, W. Cui, H. Wang, H. Zhang, Construction of dual-biofunctionalized chitosan/collagen scaffolds for simultaneous neovascularization and nerve regeneration, Research 2020. https://doi.org/10.34133/2020/2603048, 2020.
[19] P. Carmeliet, M. Tessier-Lavigne, Common mechanisms of nerve and blood vessel wiring, Nature 436 (7048) (2005) 193–200, https://doi.org/10.1038/nature03875.
[20] S. Oh, S.B. Seo, G. Kim, S. Batsukh, K.H. Son, K. Byun, Poly-D,L-Lactic acid stimulates angiogenesis and collagen synthesis in aged animal skin, Int. J. Mol. Sci. 24 (9) (2023) 7986, https://doi.org/10.3390/ijms24097986.
[21] M. Zhang, R. Lin, X. Wang, J. Xue, C. Deng, C. Feng, H. Zhuang, J. Ma, C. Qin, L. Wan, J. Chang, C. Wu, 3D printing of Haversian bone-mimicking scaffolds for multicellular delivery in bone regeneration, Sci. Adv. 6 (12) (2020) eaaz6725, https://doi.org/10.1126/sciadv.aaz6725.
[22] H. Zhang, C. Qin, M. Zhang, Y. Han, J. Ma, J. Wu, Q. Yao, C. Wu, Calcium silicate nanowires-containing multicellular bioinks for 3D bioprinting of neural-bone constructs, Nano Today 46 (2022) 101584, https://doi.org/10.1016/j.nantod.2022.101584.
[23] C. Deng, Q. Yang, X. Sun, L. Chen, C. Feng, J. Chang, C. Wu, Bioactive scaffolds with Li and Si ions-synergistic effects for osteochondral defects regeneration, Appl. Mater. Today 10 (2018) 203–216, https://doi.org/10.1016/j.apmt.2017.12.010.
[24] F. Lv, J. Wang, P. Xu, Y. Han, H. Ma, H. Xu, S. Chen, J. Chang, Q. Ke, M. Liu, Z. Yi, C. Wu, A conducive bioceramic/polymer composite biomaterial for diabetic wound healing, Acta Biomater. 60 (2017) 128–143, https://doi.org/10.1016/j.actbio.2017.07.020.
[25] H. Li, J. Chang, Bioactive silicate materials stimulate angiogenesis in fibroblast and endothelial cell co-culture system through paracrine effect, Acta Biomater. 9 (6) (2013) 6981–6991, https://doi.org/10.1016/j.actbio.2013.02.014.
[26] T. Tian, Y. Han, B. Ma, C. Wu, J. Chang, Novel Co-akermanite ($Ca_2CoSi_2O_7$) bioceramics with the activity to stimulate osteogenesis and angiogenesis, J. Mat. Chem. B 3 (33) (2015) 6773–6782, https://doi.org/10.1039/c5tb01244a.
[27] T. Tian, C. Wu, J. Chang, Preparation and in vitro osteogenic, angiogenic and antibacterial properties of cuprorivaite ($CaCuSi_4O_{10}$, Cup) bioceramics, RSC Adv. 6 (51) (2016) 45840–45849, https://doi.org/10.1039/c6ra08145b.
[28] J. Ma, C. Qin, J. Wu, H. Zhang, H. Zhuang, M. Zhang, Z. Zhang, L. Ma, X. Wang, B. Ma, J. Chang, C. Wu, 3D printing of strontium silicate microcylinder-containing multicellular biomaterial inks for vascularized skin regeneration, Adv. Healthc. Mater. 10 (16) (2021) 2100523, https://doi.org/10.1002/adhm.202100523.
[29] J. Ma, J. Wu, H. Zhang, L. Du, H. Zhuang, Z. Zhang, B. Ma, J. Chang, C. Wu, 3D printing of diatomite incorporated composite scaffolds for skin repair of deep burn wounds, Int. J. Bioprinting 8 (3) (2022) 163–175, https://doi.org/10.18063/ijb.v8i3.580.
[30] W.P. Ma, H.S. Ma, P.F. Qiu, H.J. Zhang, Z.B. Yang, B. Ma, J. Chang, X. Shi, C.T. Wu, Sprayable beta-FeSi2 composite hydrogel for portable skin tumor treatment and wound healing, Biomaterials 279 (2021) 121225, https://doi.org/10.1016/j.biomaterials.2021.121225.
[31] L. Liu, Y. Liu, C. Feng, J. Chang, R. Fu, T. Wu, F. Yu, X. Wang, L. Xia, C. Wu, B. Fang, Lithium-containing biomaterials stimulate bone marrow stromal cell-derived exosomal miR-130a secretion to promote angiogenesis, Biomaterials 192 (2019) 523–536, https://doi.org/10.1016/j.biomaterials.2018.11.007.
[32] P. Cannata-Ortiz, C. Gracia, Y. Aouad, A. Barat, M. Angel Martinez-Gonzalez, G. Rossello, C. Martin-Cleary, B. Fernandez-Fernandez, L. Requena, A. Ortiz, Small vessel microembolization and acute glomerulonephritis following infection of aesthetic filler implants, Diagn. Pathol. 11 (2016) 2, https://doi.org/10.1186/s13000-016-0453-y.
[33] M.R. Ghahramani, A.A. Garibov, T.N. Agayev, M.A. Mohammadi, A novel way to production yttrium glass microspheres for medical applications, Glass Phys. Chem. 40 (3) (2014) 283–287, https://doi.org/10.1134/s1087659614030055.
[34] K.M.Z. Hossain, U. Patel, I. Ahmed, Development of microspheres for biomedical applications: a review, Prog. Biomater. 4 (1) (2015) 1–19, https://doi.org/10.1007/s40204-014-0033-8.
[35] Y. Hwang, J.S. Lee, H. An, H. Oh, D. Sung, G. Tae, W.I. Choi, Hydroxyapatite-embedded levan composite hydrogel as an injectable dermal filler for considerable enhancement of biological efficacy, J. Ind. Eng. Chem. 104 (2021) 491–499, https://doi.org/10.1016/j.jiec.2021.08.040.
[36] W.I. Choi, Y. Hwang, A. Sahu, K. Min, D. Sung, G. Tae, J.H. Chang, An injectable and physical levan-based hydrogel as a dermal filler for soft tissue augmentation, Biomater. Sci. 6 (10) (2018) 2627–2638, https://doi.org/10.1039/c8bm00524a.
[37] L.H. Chen, J.F. Xue, Z.Y. Zheng, M. Shuhaidi, H.E. Thu, Z. Hussain, Hyaluronic acid, an efficient biomacromolecule for treatment of inflammatory skin and joint diseases: a review of recent developments and critical appraisal of preclinical and

clinical investigations, Int. J. Biol. Macromol. 116 (2018) 572–584, https://doi.org/10.1016/j.ijbiomac.2018.05.068.
[38] L. Mao, L. Xia, J. Chang, J. Liu, L. Jiang, C. Wu, B. Fang, The synergistic effects of Sr and Si bioactive ions on osteogenesis, osteoclastogenesis and angiogenesis for osteoporotic bone regeneration, Acta Biomater. 61 (2017) 217–232, https://doi.org/10.1016/j.actbio.2017.08.015.
[39] M. Xing, X. Wang, E. Wang, L. Gao, J. Chang, Bone tissue engineering strategy based on the synergistic effects of silicon and strontium ions, Acta Biomater. 72 (2018) 381–395, https://doi.org/10.1016/j.actbio.2018.03.051.
[40] C. Wu, W. Fan, M. Gelinsky, Y. Xiao, P. Simon, R. Schulze, T. Doert, Y. Luo, G. Cuniberti, Bioactive SrO-SiO2 glass with well-ordered mesopores: characterization, physiochemistry and biological properties, Acta Biomater. 7 (4) (2011) 1797–1806, https://doi.org/10.1016/j.actbio.2010.12.018.
[41] J. Hao, X. Yu, K. Tang, X. Ma, H. Lu, C. Wu, 3D modular bioceramic scaffolds for the investigation of the interaction between osteosarcoma cells and MSCs, Acta Biomater. (2024), https://doi.org/10.1016/j.actbio.2024.06.016.
[42] H. Zhang, M. Zhang, D. Zhai, C. Qin, Y. Wang, J. Ma, H. Zhuang, Z. Shi, L. Wang, C. Wu, Polyhedron-like biomaterials for innervated and vascularized bone regeneration, Adv. Mater. (2023) 2302716, https://doi.org/10.1002/adma.202302716.
[43] S.-W. Kim, H. Kim, H.-J. Cho, J.-U. Lee, R. Levit, Y.-s. Yoon, Human peripheral blood-derived CD31(+) cells have robust angiogenic and vasculogenic properties and are effective for treating ischemic vascular disease, J. Am. Coll. Cardiol. 56 (7) (2010) 593–607, https://doi.org/10.1016/j.jacc.2010.01.070.
[44] X. Ding, W. Zhang, P. Xu, W. Feng, X. Tang, X. Yang, L. Wang, L. Li, Y. Huang, J. Ji, D. Chen, H. Liu, Y. Fan, The regulatory effect of braided silk fiber skeletons with differential porosities on in vivo vascular tissue regeneration and long-term patency, Research 2022, 11, https://doi.org/10.34133/2022/9825237, 2022.
[45] S. Udenfriend, Formation of hydroxyproline in collagen, Science 152 (3727) (1966) 1335–1340, https://doi.org/10.1126/science.152.3727.1335.
[46] X. Liu, H. Wu, M. Byrne, S. Krane, R. Jaenisch, Type III collagen is crucial for collagen I fibrillogenesis and for normal cardiovascular development, Proc. Natl. Acad. Sci. U. S. A. 94 (5) (1997) 1852–1856, https://doi.org/10.1073/pnas.94.5.1852.
[47] J.N. Clore, I.K. Cohen, R.F. Diegelmann, Quantitation of collagen types I and III during wound healing in rat skin, Proc. Soc. Exp. Biol. Med. 161 (3) (1979) 337–340, https://doi.org/10.3181/00379727-161-40548.
[48] P.K. Mays, J.E. Bishop, G.J. Laurent, Age-related changes in the proportion of types I and III collagen, Mech. Ageing Dev. 45 (3) (1988) 203–212, https://doi.org/10.1016/0047-6374(88)90002-4.
[49] J. Huang, X. Lei, Z. Huang, Z. Rong, H. Li, Y. Xie, L. Duan, J. Xiong, D. Wang, S. Zhu, Y. Liang, J. Wang, J. Xia, Bioprinted gelatin-recombinant type III collagen hydrogel promotes wound healing, Int. J. Bioprinting 8 (2) (2022) 13–24, https://doi.org/10.18063/ijb.v8i2.517.